On Latent Fingerprint Enhancement

Soweon Yoon[a], Jianjiang Feng[a], and Anil K. Jain*[a,b]

[a]Department of Computer Science and Engineering, Michigan State University, East Lansing, MI 48824, USA;

[b]Department of Brain and Cognitive Engineering, Korea University, Anam-dong, Seongbuk-gu, Seoul 136-713, Korea

ABSTRACT

Automatic feature extraction in latent fingerprints is a challenging problem due to poor quality of most latents, such as unclear ridge structures, overlapped lines and letters, and overlapped fingerprints. We proposed a latent fingerprint enhancement algorithm which requires manually marked region of interest (ROI) and singular points. The core of the proposed enhancement algorithm is a novel orientation field estimation algorithm, which fits orientation field model to coarse orientation field estimated from skeleton outputted by a commercial fingerprint SDK. Experimental results on NIST SD27 latent fingerprint database indicate that by incorporating the proposed enhancement algorithm, the matching accuracy of the commercial matcher was significantly improved.

Keywords: Latent fingerprints, orientation field estimation, fingerprint image enhancement, singularity

1. INTRODUCTION

Fingerprints have been routinely used as a method for person identification for more than a century. One of the irreplaceable functionality of fingerprint recognition is its capability to link partial prints found at crime scenes to suspects whose fingerprints are previously enrolled in a large database of rolled fingerprints. These partial prints, called latent fingerprints or simply latents, are lifted from surfaces of objects that are inadvertently touched or handled by a person. Lifting of latents involves a complicated process that can range from simply photographing the print to more complex dusting or chemical processing[1]. Compared to plain or rolled fingerprints (see Figure 1), which are captured by inking methods or livescan devices in an attended mode, latent fingerprints are smudgy and blurred, capture only a small finger area, and have large nonlinear distortion due to pressure variations. Due to their poor quality and small area, latents have a significantly smaller number of minutiae compared to rolled or plain prints (the average number of minutiae in NIST SD27[9] database images is 21 for latents versus 106 for the corresponding rolled prints).
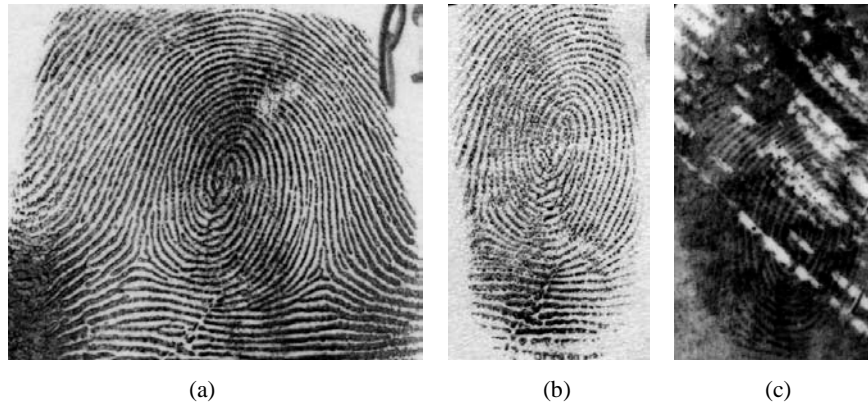

(a)   (b)   (c)

Figure 1. Three types of fingerprint images. (a) Rolled, (b) plain and (c) latent fingerprints of the same finger (Latent #158) in NIST SD27.

* jain@cse.msu.edu; phone 1 517 355 9282

Before the introduction of Automatic Fingerprint Identification systems (AFIS), latents were manually matched against full prints (rolled or plain) by latent examiners through a procedure now referred to as ACE-V, namely, *analysis*, *comparison*, *evaluation* and *verification*[2]. Unlike full print (rolled or plain) to full print matching, which is somewhat facilitated by fingerprint pattern class or type, manually matching a latent print against a large gallery is not feasible. Generally, latents are only matched against full prints of a small number of suspects who are identified from other means (e.g. gender, ethnicity, age, etc.).

The emergence of Automated Fingerprint Identification Systems (AFIS) significantly improved the speed of fingerprint identification and made latent identification against a large fingerprint database feasible. After over thirty years of development, tremendous advances have been made in both the throughput and accuracy of full print to full print matching. The results of Fingerprint Vendor Technology Evaluation (FpVTE) in 2003[3] showed that the most accurate commercial fingerprint matchers achieved an impressive rank-1 identification rate of more than 99.4% on a database of 10,000 plain fingerprint images. The US-VISIT IDENT system can search fingerprints of a visitor to the United States against a watch list of millions of subjects in a few seconds[4]. However, this throughput and accuracy of fingerprint identification for rolled/plain prints has not yet been realized for latent identification. Due to the generally poor quality of latents, latent identification module in AFIS typically works in a semi-automatic mode for the sake of identification accuracy. A typical scenario is that an expert first manually marks features in a latent, launches AFIS search, and finally reviews the candidate list returned by AFIS to identify the true mate (if present). Extensive manual intervention is needed in both feature marking and review stages. In spite of this, latent matching accuracy is still not satisfactory. It was reported that the rank-1 identification rate of the FBI's IAFIS is about 54% on a large database of more than 40 million subjects[5]. In our recent work[10], a rank-1 accuracy of 79.5% was obtained in matching 258 latents in NIST SD27 against 2,258 rolled prints.

In the long run, "Lights-Out"[1] latent identification capability is desirable. Consider the following two scenarios: (i) a patrol officer wants to check fingerprints of a suspect against latent fingerprints from unsolved cases; (ii) a crime scene specialist hopes to identify latents lifted at a crime scene in the field. In both these cases, it would be desirable to get a quick (real time) response to the query. To understand and advance the state of the art in automatic latent feature extraction and matching, NIST has been conducting a multi-phase project on Evaluation of Latent Fingerprint Technologies (ELFT)[6]. The rank-1 accuracy of the most accurate system in ELFT Phase I was ~80% in matching 100 latents against 10,000 rolled prints[7]. Much higher accuracies were reported in ELFT Phase II organized shortly after Phase I. The rank-1 accuracy of the most accurate system in Phase II is 97.2% in matching 835 latents against a galley of 100,000 rolled prints[8]. Unfortunately, Phase I and Phase II accuracies cannot be compared because different databases were used in the two evaluations. Further, the Phase II accuracy does not reflect the performance in field applications, since the latents used in Phase II are of very good quality. Figure 2 shows three latents of different quality in NIST SD27.
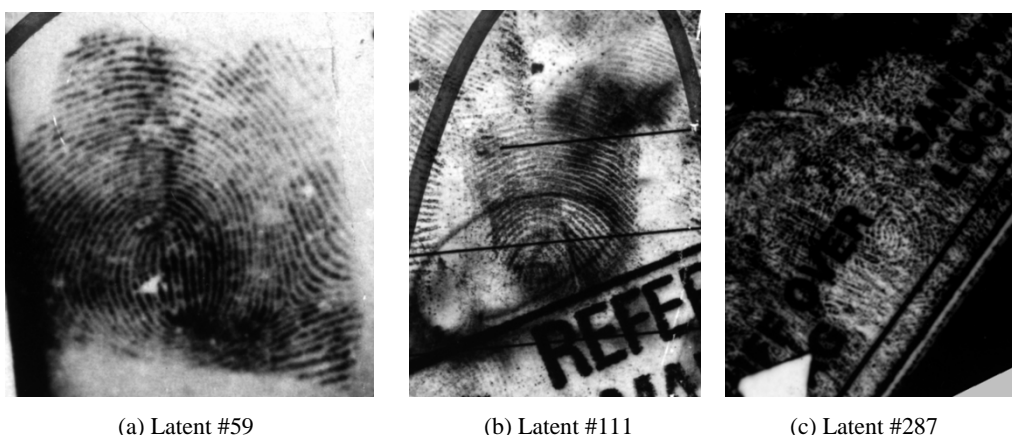

(a) Latent #59   (b) Latent #111   (c) Latent #287

Figure 2. Latent fingerprints of three different quality levels in NIST SD27. (a) Good, (b) Bad, and (c) Ugly.

---

[1] In a "Lights-Out" fingerprint identification system, manual feature marking is not required and only one mated fingerprint or no mate is returned by the system.

It is our opinion that research efforts in latent fingerprint identification should be focused on reducing the necessary manual input while at the same time preserving the matching accuracy, rather than on completely eliminating manual input. This opinion is supported by the following facts: (i) latent matching accuracy is still the major concern of law enforcement agencies, (ii) currently manual latent feature marking is very labor extensive, and (iii) state of the art "Lights-Out" latent identification systems cannot yet offer satisfactory accuracy for most latents of casework quality.

In current practice, latent examiners are required to mark minutiae and optionally singular points (core/delta)[11]. Marking these features is generally less time-consuming and requires less expertise than marking minutiae, which are required by the current practice. In this paper, we assume that the manually marked features are Region of Interest (ROI) and singular points. Therefore, this procedure will not only improve the throughput of latent identification system, but reduce the cost as well, since human expertise and time are expensive. We proposed an orientation field estimation algorithm, which takes skeleton images generated by a commercial fingerprint SDK, Neurotechnology VeriFinger[12], and manually marked singular points as input. Gabor filters were used to enhance latent images. To test the proposed enhancement algorithm, we combined it with VeriFinger matcher and conducted experiments on a public domain fingerprint database, NIST SD27.

2. LATENT FINGERPRINT ENHANCEMENT

2.1 Overview

The purpose of an enhancement algorithm is to improve the clarity of the ridge structures and therefore make the subsequent processing, such as minutiae extraction and matching algorithm, insensitive to the quality of fingerprint images. Fingerprint enhancement is especially important to latent images, due to their poor quality. Local ridge pattern in fingerprints can be approximated well by a 2D sinusoid wave. Based on this fact, 2D Gabor filters[15] have been successfully used for fingerprint enhancement. Gabor filters consist of two important parameters: local ridge orientation and frequency. With proper choice of these parameters, Gabor filtering can connect broken ridges and separate joined ridges. However, when the parameters are incorrect, true ridges may be weakened and spurious ridges may be strengthened after filtering. Hence, a reliable estimation of local ridge orientation and frequency is very important to fingerprint enhancement. Compared to frequency, ridge orientation is even more important, as the range of possible ridge frequency values is small for adult fingerprints and ridge frequency is often estimated after ridge orientation is known[15]. For this reason, in this paper, we focus on the estimation of orientation field in latent images.

Due to its importance, orientation field estimation is a popular topic in fingerprint recognition literature. Most orientation field estimation algorithms[14][15] consist of two steps: initial estimation using a gradient-based method followed by regularization. The regularization may be done by a simple weighted averaging filter or more complicated model-based methods[15]. To make regularization effective, it is better to use only reliable initial estimate or to give it larger weight. However, very limited information is available at this stage to estimate the reliability of initial estimate. To overcome this limitation, we estimate a coarse orientation field from skeleton image generated by a commercial SDK. This coarse

- Latent Image
- ROI (manual)
- Singular Points (manual)
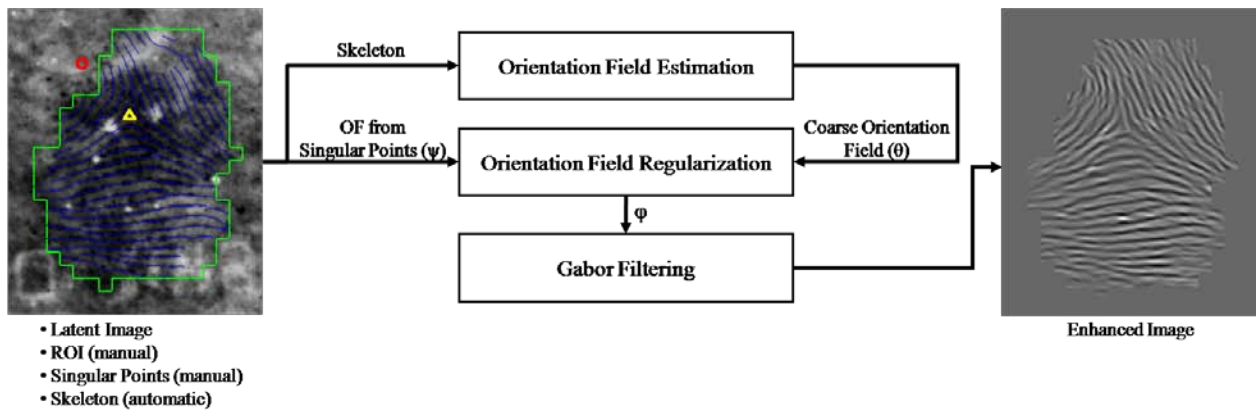- Skeleton (automatic)

Figure 3. Flowchart of the proposed latent enhancement algorithm.

orientation field is further regularized by fitting an orientation field model to it. The flowchart of the proposed latent enhancement algorithm is shown in Figure 3. In the following subsections, we first explain manual input and then describe the coarse estimation and regularization of orientation field.

2.2 Manual Input

Level-1 fingerprint features include ridge orientation field and singular points. Ridge orientation field can be marked at block level (usually the size of block is 16 by 16 pixels). A possible scenario for manual orientation field marking is that the gradients of the local blocks give initial estimate of the orientation field and examiners can then make a correction in the blocks with wrong orientation field. However, latent fingerprints are largely corrupted by complex background noise and the ridge structures are not clearly visible to human eye. Therefore, manual orientation field marking requires a high level of attention by the examiners.

Compared to orientation field marking, singular points are easy for examiners to mark manually since the number of singularities is small (at most four in a fingerprint) and their locations are easy to identify. Based on a thorough investigation of fingerprints, we could find two constraints on singularities in the fingerprints: (i) the numbers of cores and deltas in a finger are the same, and (ii) the total number of singular points in a fingerprint is zero, two or four. For example, loop and tented arch type of fingerprints have one core and one delta; double-loop and whorl type of fingerprints have two cores and two deltas; arch type of fingerprints has no singularity.

We assume that latent examiners can provide the following information to automatic fingerprint matcher: (i) latent fingerprint region in the image or the region of interest (ROI) and (ii) singular points. When latent examiners manually mark the singular points, we assume that they follow two rules:

- If the latent does not contain singular points, no singular points are marked. In other words, we treat a latent as plain arch unless contradictory information is present.

- If the number of real singular points in the ROI is odd, paired singular points outside of the ROI, which is called virtual singular points, are marked with the best guess in order to satisfy the constraints on singularity (i.e. the number of cores and deltas are the same and the total number of singular points is one of 0, 2, and 4).

See Figure 4 for three examples that contain no singular points, only real singular points, and both real and virtual singular points, respectively.

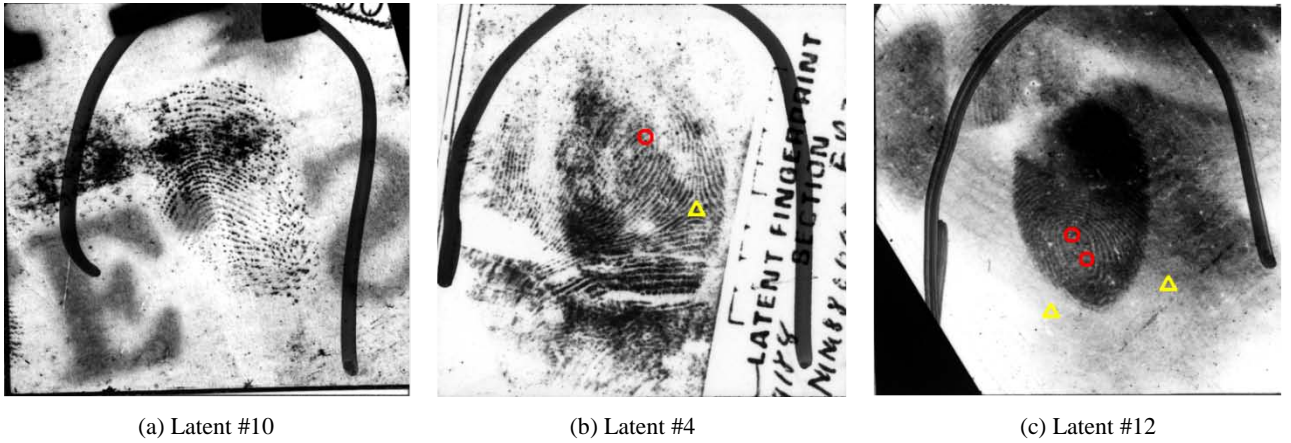| (a) Latent #10 | (b) Latent #4 | (c) Latent #12 |

Figure 4. Singular points of the latent fingerprints. (a) No singular points, (b) only real singular points, and (c) both real and virtual singular points. Circles denote cores and triangles denote deltas.
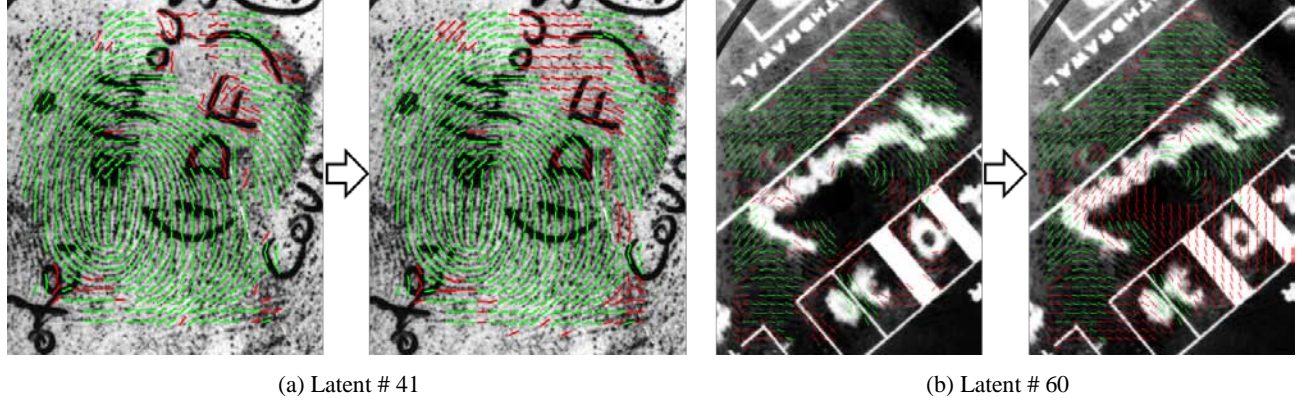
(a) Latent # 41 (b) Latent # 60

Figure 5. Coarse orientation field estimation. Left images: green lines are reliable (coherent) orientation field and red lines are unreliable orientation field. Right images: green lines are reliable orientation field and red lines are interpolated orientation field from reliable blocks.

2.3 Coarse Estimation of Orientation Field

In general, latent fingerprints are corrupted by complex background noise or have unclear ridge structures. Instead of estimating the coarse orientation field directly from the image, we utilize skeleton provided by a commercial software, and then correct wrong ridge orientations in the noisy areas.

The orientation field can be represented in complex plane with doubled angle:

$$U(x,y) = \cos(2\theta(x,y)) + j\sin(2\theta(x,y)), \tag{1}$$

where $\theta(x,y)$ is the orientation field from the skeleton and $U(x,y)$ is a representation of the angle in complex domain. Reliable blocks where the orientation fields are coherent with surrounding blocks are distinguished from the initial orientation field. The orientation field in unreliable blocks is estimated by interpolating the orientation field in reliable blocks. Real and imaginary part of $U(x,y)$ in unreliable blocks are independently estimated from those in reliable blocks, and then converted to the angles. Figure 5 shows the orientation field from the skeleton and the corrected orientation field in unreliable blocks.

2.4 Regularization of Orientation Field

A zero-pole model[13] describes an ideal orientation field of the fingerprint by singular points. A rational polynomial function in complex plane determines the ridge orientation at a point $z = x + jy$ by:

$$\psi(z) = \frac{1}{2}\arg\left[e^{j2\theta_\infty}\frac{P(z)}{Q(z)}\right], \tag{2}$$

where $P(z) = (z - z_{c_1})(z - z_{c_2})\cdots(z - z_{c_m})$, $Q(z) = (z - z_{d_1})(z - z_{d_2})\cdots(z - z_{d_m})$, $\{z_{c_i}\}_{1\le i\le m}$ and $\{z_{d_i}\}_{1\le i\le m}$ are the locations of the cores and deltas, and θ_∞ is the orientation field at infinity. This zero-pole model requires a complete set of singular points of a fingerprint. We need to estimate θ_∞ when the fingerprint is rotated in the image.

An inherent limitation of the zero-pole model is that this model can not represent arch type of fingerprints which does not have any singular points. In addition, since the orientation field estimated by this model depends only on the locations of singular points, this model can not reflect local ridge orientation of the real fingerprints in detail.

Zhou and Gu[14] extend zero-pole model to represent local ridge orientation by combining it with a polynomial function. The zero-pole model is used to represent the global orientation field due to known singular points and the polynomial function represents ridge details. However, the fingerprint impressions are usually a part of the actual fingerprint unless

the fingerprint is scanned by 'nail-to-nail' method. Therefore, the zero-pole model using only known singular points in the image cannot take into account all the effects of all the singularities to the orientation field. As a result, the polynomial function should be of high order to describe large curvature of the orientation field.

In our model, the global orientation field consists of two parts: (i) the orientation field due to all the singular points, including real singular points in the ROI as well as virtual singular points, $\psi(x, y)$, and (ii) polynomial model for ridge details which reflects fingerprint rotation and skin distortion, $\delta(x, y)$. $\psi(x, y)$ depends on types and spatial distribution of singular points. Figure 6 shows the orientation field by singular points.

The orientation field model, $\phi(x, y)$, can be written as:

$$\phi(x, y) = \psi(x, y) + \delta(x, y),\tag{3}$$

where $\psi(x, y)$ is the orientation field from all possible singular points and $\delta(x, y)$ is the polynomial model. $\delta(x, y)$ is estimated by minimizing $\sum_{(x,y)\in R}|(\theta(x, y) - \psi(x, y)) - \delta(x, y)|^2$ using least-squares estimation, where $\theta(x, y)$ is the coarse orientation field estimated from the image and R denotes the ROI. In our model, we used a second order polynomial function for $\delta(x, y)$, which is the minimal order of the polynomial function to represent curves. The polynomial function with low order only needs to estimate a few parameters. In particular, when the order of polynomial function is 2, the number of parameters to be estimated is 6 (since $\delta(x, y) = a_0 + a_1 x + a_2 y + a_3 x^2 + a_4 xy + a_5 y^2$). In addition, it is robust to complex noise present in the latent images. Figure 7 shows the orientation field estimation of the latent fingerprint using the proposed method.
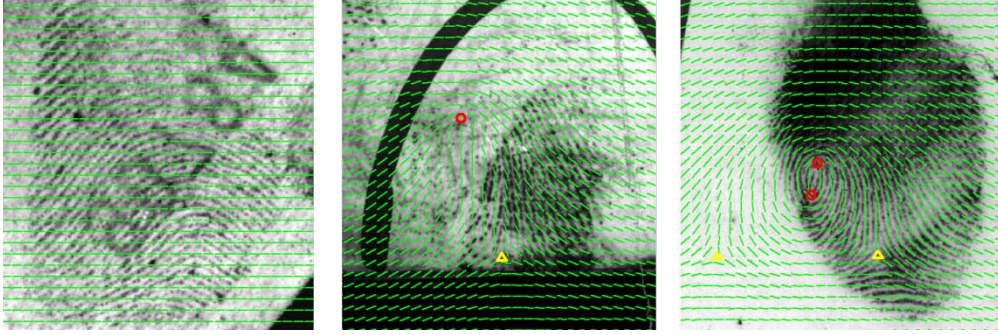

Figure 6. Orientation field from singular points. (a) No real singular point is present, (b) a real delta and its corresponding virtual core are marked, and (c) two real cores, one real delta and the corresponding virtual delta are marked.
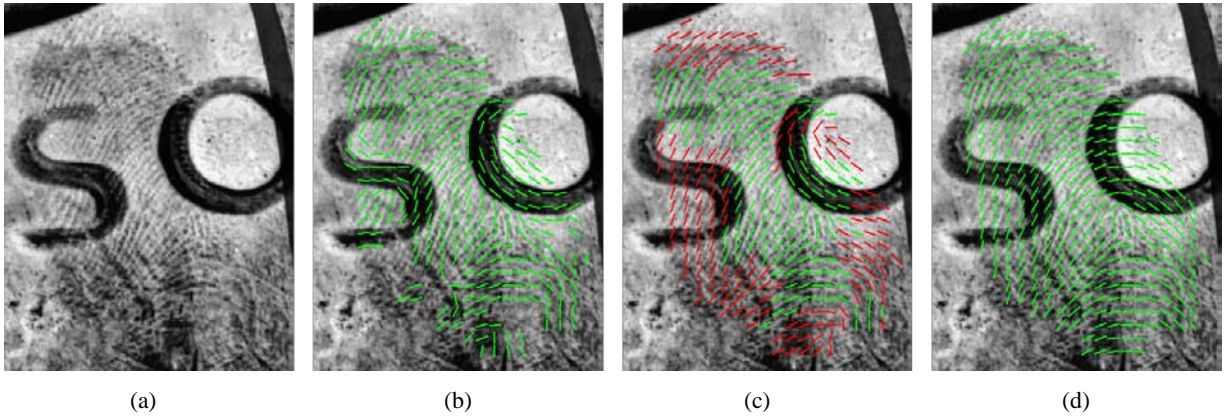

| (a) | (b) | (c) | (d) |

Figure 7. Orientation field estimation. (a) Input image (Latent #57), (b) orientation field from skeleton, (c) orientation field corrected (green: reliable orientation field, red: estimated orientation field from reliable blocks), (d) orientation field regularized by the proposed model.

3. EXPERIMENTAL RESULTS

3.1 Database

The experiments were conducted on NIST SD27 database[9] which contains 258 latent fingerprints and their corresponding rolled prints at 500 ppi. This is the only public domain database available containing mated latent and rolled prints. These 258 latent prints were classified by latent examiners into three classes based on their quality, namely: Good, Bad and Ugly. There are 88 "Good", 85 "Bad" and 85 "Ugly" latent images in the database.

3.2 Matching Performance

We conducted experiments by matching 258 latents against 258 rolled prints for four types of manual input (in the increasing order of labor):

- Manually marked ROI. Minutiae are automatically extracted in the ROI using VeriFinger SDK 4.2[12].

- Manually marked ROI and singular points. Orientation field is first estimated using the proposed algorithm; fingerprint is then enhanced using Gabor filtering and minutiae are automatically extracted in the enhanced image using VeriFinger SDK. This is the scenario which the proposed enhancement algorithm is designed for.

- Manually marked ROI and orientation field. The orientation field is directly used in Gabor filtering and minutiae are then automatically extracted in the enhanced image using VeriFinger SDK.

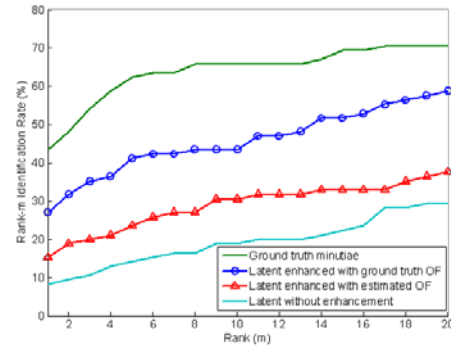- Manually marked minutiae are directly used by VeriFinger matcher.
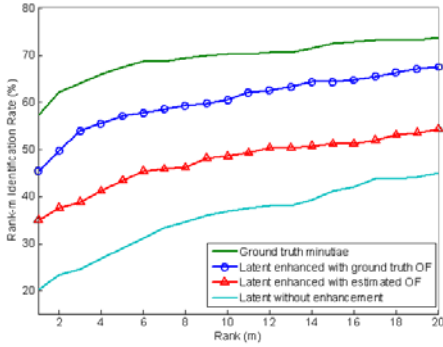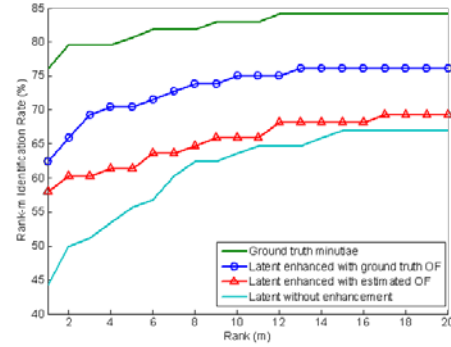
(a) All latents   (b) "Good" latents
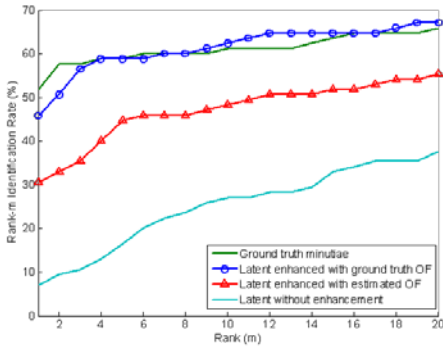
(c) "Bad" latents   (d) "Ugly" latents

Figure 8. CMC curves of latent matching in four scenarios. 258 latents were matched to 258 rolled prints in NIST SD27. (a) All, (b) good, (c) bad, (d) ugly latents.

The Cumulative Match Characteristic (CMC) curves of these four types of input are shown in Figure 8(a). As expected, the matching accuracy is consistent with the labor of manual input. The highest accuracy is obtained when minutiae are manually marked and the worst accuracy is obtained when only ROI is provided. The effectiveness of the proposed enhancement algorithm is validated by the fact that matching accuracy is improved due to manually marked singular points. But, the higher accuracy of using manually marked orientation field indicates that the proposed orientation field estimation algorithm needs to be improved.

Figure 8 (b-d) show CMC curves of four types of input for good, bad and ugly latents, respectively. We observed that

- The proposed enhancement algorithm leads to improved matching accuracy for all three categories.

- For bad quality latents, image enhancement with ground truth orientation field achieved almost the same performance as ground truth minutiae.
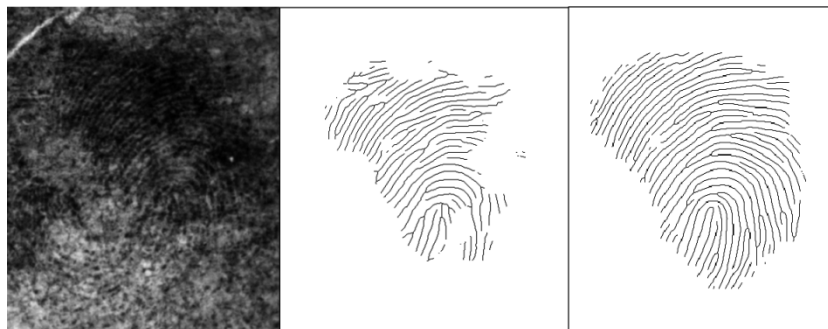
The examples in clearly show the effect of the proposed enhancement algorithm. Due to the enhancement algorithm, more ridges can be correctly extracted in poor quality area.

(a) Latent #32
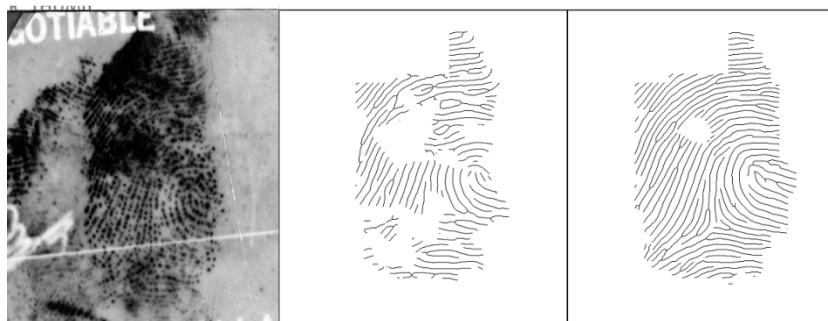
(b) Latent #164

(c) Latent #227

Figure 9. Skeleton images without and with the proposed enhancement. Left: latent fingerprint, center: skeleton without enhancement, and right: skeleton with enhancement. (a) Good latent (matching score was improved from 4 to 67), (b) bad latent (from 4 to 95), and (c) ugly latent (from 0 to 23).

4. CONCLUSIONS AND FUTURE DIRECTIONS

Increasing deployment of fingerprint recognition systems in civilian and governmental applications has resulted in more and more fingerprints being collected from citizens who were not required to pass fingerprint check in the past, such as an applications for certain jobs, international border crossing at a port of entry, and a suspect stopped by a patrol officer, etc. Matching these new fingerprints to latents of unsolved cases has the potential of solving more "cold cases". This practice makes shortening the response time of latent identification an urgent issue. While fully automatic latent identification is desirable in the long term, a more practical goal in the interim is to reduce manual input while preserving the matching accuracy.

In this paper, we proposed a latent fingerprint enhancement algorithm which only requires manually marked ROI and singular points. The core of the proposed enhancement algorithm is an orientation field estimation algorithm, which fits an orientation field model to the coarse orientation field estimated from skeleton provided by a commercial fingerprint SDK. Experimental results on NIST SD27 indicate that using singular points is beneficial to minutiae extraction, leading to improved matching accuracy.

We plan to extend the current work along two directions.

- Define more effective manual inputs. For some latents, singular points may not be the most effective input. For example, the singular region may be of good quality, or the latents may not contain singular points. In these cases, inputting a curve indicating the ridge flow in some critical regions (such as regions with overlapped lines or letters) may be more effective for estimating the orientation field.

- Reduce manual input even further. Currently, region of interest (ROI) is specified by a polygon that requires inputting all the vertices. A more efficient input method for specifying ROI is that the user inputs a circular region, which roughly covers the ROI, and then the algorithm automatically locates the accurate boundary of the ROI.

ACKNOWLEDGMENTS

REFERENCES

[1] Lee, H. C. and Gaensslen, R. E., [Advances in Fingerprint Technology], CRC Press (2001).

[2] Ashbaugh, D. R., [Quantitative-Qualitative Friction Ridge Analysis: An Introduction to Basic and Advanced Ridgeology], CRC Press (1999).

[3] Wilson, C. *et al.*, "Fingerprint Vendor Technology Evaluation 2003: Summary of Results and Analysis Report," NISTIR 7123, June (2004) http://fpvte.nist.gov/report/ir_7123_analysis.pdf.

[4] Wilson, C. L., Garris, M. D., and Watson, C. I., "Matching Performance for the US-VISIT IDENT System Using Flat Fingerprints," NISTIR 7110, May (2004).

[5] Dvornychenko, V. N. and Garris, M. D., "Summary of NIST Latent Fingerprint Testing Workshop," NISTIR 7377, November (2006) http://fingerprint.nist.gov/latent/ir_7377.pdf.

[6] "Evaluation of Latent Fingerprint Technologies 2007," http://fingerprint.nist.gov/latent/elft07/.

[7] NIST, "Summary of the Results of Phase I ELFT Testing," September (2007) http://fingerprint.nist.gov/latent/elft07/phase1_aggregate.pdf.

[8] Indovina, M. *et al.*, "ELFT Phase II - An Evaluation of Automated Latent Fingerprint Identification Technologies," NISTIR 7577, April (2009).

[9] NIST Special Database 27, "Fingerprint Minutiae from Latent and Matching Tenprint Images," http://www.nist.gov/srd/nistsd27.htm.

[10] Jain, A. K., Feng, J., Nagar, A. and Nandakumar, K., "On Matching Latent Fingerprints," CVPR Workshop on Biometrics, 1-8 (2008).

[11] FBI Electronic Fingerprint Transmission Specification, http://www.fbi.gov/hq/cjisd/iafis/efts71/efts71.pdf.

[12] Neurotechnology VeriFinger, http://www.neurotechnology.com/vf_sdk.html.

[13] Sherlock, B.G., and Monro, D.M., "A model for interpreting fingerprint topology," Pattern Recognition, 26(7), 1047-1055 (1993).

[14] Zhou, J., and Gu, J., "Modeling orientation fields of fingerprints with rational complex functions," Pattern Recognition, 37(2), 389-391 (2004).

[15] Hong, L., Wang, Y. and Jain, A.K., "Fingerprint Image Enhancement: Algorithm and Performance Evaluation," IEEE Trans. on Pattern Analysis and Machine Intelligence, 20(8), 777-789 (1998).